

Bubble Entrapment During Water Drop Impacts

D.E. Cole ¹ and J.L. Liow ¹

¹Mechanical Engineering Discipline, School of Engineering
 James Cook University, Qld, 4811 AUSTRALIA

Abstract

In the splash of a liquid drop on a deep pool of water, bubble entrapment occurs over a limited range of Froude number. Using high speed video photography at framing rates between 10000-100000 fps, the bubble entrapment regime was studied for water drops impacting on a deep pool of water. It is known that a high speed jet accompanies the entrapment of a bubble. In this study it was found that preceding the appearance of the high speed jet, a series of high speed droplets, having diameters up to a magnitude smaller than droplet previously observed, appears. The speed of these droplets were 50% higher than those formed from the high speed jets. We believe that these smaller high speed droplets were the result of a focusing of the ejecta sheet into a thin high speed jet. This thin high speed jet breaks up rapidly on formation and cannot be observed above the bath free surface. In conjunction with the upward high speed jet, an entrapped bubble was found to be expelled downwards from the cavity with a high speed downward jet of liquid penetrating into the bubble. If the high speed downward jet penetrated far enough into the bubble, such that its length exceeded Rayleighs wavelength for instability, it broke up to form a single drop within the bubble. The entrapped drop would then bounce around inside the bubble before the drop coalesced with the bulk liquid through a coalescence cascade with a geometric similarity given by $We = 8$.

Introduction

The impact of a water drop on a deep pool of water has been studied for almost a hundred years, beginning with the spark photography of Worthington [13]. Applications of liquid-liquid impacts include gas injection metallurgy, fire suppression systems [5] and behaviour of the worlds oceans. When the water drop impacts, a range of phenomena subsequent to the impact have been observed. The occurrence of these phenomena have been detailed by Rein [9] and Liow [2], and shown to be primarily dependent on the Froude number (defined as $Fr = u^2/(gd)$) and to a lesser extent, the Weber number (defined as $We = \rho u^2 d/\sigma$). At low Froude numbers, the water drop coalesces with the pool and forms a vortex ring that is propagated into the pool water. At higher Froude numbers, a cavity is formed after impact. With still increasing Froude numbers, the cavity formed collapses to entrap an air bubble with the formation of a high speed water jet; this connection was first observed by Rein [9]. Subsequently, based on physical arguments, Oguz and Prosperetti [7] derived scalings for the lower and upper limits for the occurrence of the high speed jet based on as $We \approx Fr^{1/5}$ and $We \approx Fr^{1/4}$ respectively. Fitting to experimental measurements [7], the lower and upper limits are $We = 41.3Fr^{0.179}$ and $We = 40Fr^{0.247}$. Liow [2] results suggest that the range for the formation of a high speed jet is larger than the range for the bubble entrapment, more so for the lower limit. For Froude numbers larger than those in the region where the high speed jet is found, the cavity does not entrap a bubble and a thick slow jet is formed after the cavity collapses.

The formation of the entrapped bubble occurs very rapidly, in the order of less than 1 millisecond. High speed cinematic re-

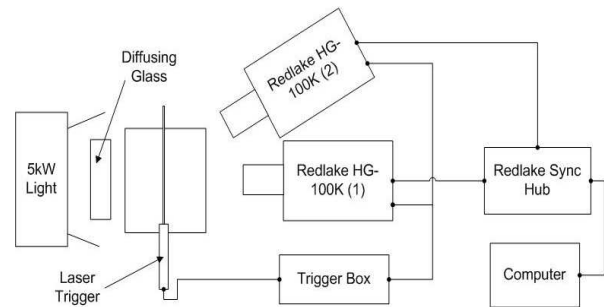


Figure 1: Schematic of the experimental apparatus.

sults at 5000 fps for two specific cases [1] show that the bubble entrapment process is not fully captured at those speeds. Their results show that the cavity base stagnates prior to bubble entrapment.

Although the events leading up to bubble entrapment is well known and published, the process of bubble entrapment is still not fully understood as the duration is extremely short. Moreover, the process of the formation of the high speed jet and the subsequent motion of the entrapped bubble has not been studied in any detail. In this paper, a high speed video study of the bubble entrapment process was conducted to capture events that have a lifetime of less than 1 ms.

Experimental

The experimental setup is shown schematically in Figure 1. Apart from the high speed video and lighting, the experimental setup uses the same equipment as that of Liow [2] where water drops of approximately 2 mm diameters are formed at regular intervals. A pair of high speed video cameras, Redlake HG-100K, are used here, to provide synchronised details above and below the water bath. The resolution of the high speed video is dependent on the framing rate, 1504×1128 pixels at 1000 fps, 512×512 at 5000 fps and 352×352 at 10000 fps with a minimum exposure of $5 \mu s$. A Nikon Micro 105 mm lens on f11 was used and positioned so that each pixel in the image represented a $12 \mu m$ square. The drops were released from different heights to vary the impact velocity. The diameter of the drop was used as the characteristic length scale and the ratio of the drop diameter to impact velocity provided the characteristic time scale. A 5kW Arri fresnel lamp was used to provide the back illumination.

Results and Discussion

The results presented here deals with specific phenomena that have not been reported or have been reported with insufficient details in the published literature.

Thin High Speed Jet

The high speed jet phenomena has generated considerable interest since Rein [9] linked the high speed jet to bubble entrapment. Zeff *et al.* [14] suggested that the high speed jet resulted

from a singularity. An early explanation by Oğuz and Prosperetti [7] suggested that this was due to the cavity base having a high momentum and was still travelling downwards while the cavity sides collapsed inwards. Liow [2] showed experimentally that the cavity base motion stagnates prior to bubble entrapment and suggested that a nonlinear capillary wave travelling down the cavity wall balances the upward momentum of the cavity base enabling the cavity sides to close in, trapping the bubble. This experimental observation was confirmed by Elmore *et al.* [1].

Figure 2 shows a sequence of drops generated from the impact of a water drop ($Fr = 110$, $We = 100$) in the region of thin high speed jet formation. On close observation, it was found that prior to the emergence of the high speed jet, a series of even smaller droplets was found to be ejected at high velocities. The small droplets did not necessarily follow the same upward trajectory as the high speed jet suggesting the presence of an initial thin high speed jet preceding the high speed jet. This thin high speed jet would be fairly short in length prior to breakup. The smallest droplets observed from this thin high speed jet occupied 1 to 2 pixels corresponding to $18 \mu\text{m}$ in diameter. The previous smallest drops resulting from the high speed jet were in the order of $70 \mu\text{m}$ [2]. The size of droplets from the thin high speed jet is below the resolution of [2] and [9] and the current measurements suggest that it could be up to an order of magnitude smaller in size. The highest speed of a thin high speed jet droplet was calculated at over 15 m/s. In comparison, previous measurement of the speed of the high speed jet have been less than 10 m/s. The thin high speed jet disappears from view within 2 ms. Morton *et al.* [6] numerical simulations of the high speed jet does not show the presence of the thin high speed jet and this could be due to the grid resolution $\approx 25 \mu\text{m}$. Although a low pressure region was identified at the cavity base where positive vorticity was generated, Morton *et al.* did not provide a pressure map for the time when the cavity wall met to entrap the bubble. The presence of high speed jets suggest that a high pressure region must form at the impact site of the walls.

Figure 2 shows that the thin high speed droplet sizes that emerge into view are not necessarily a succession of the smallest to the largest. Droplets 1 and 4 are the smallest but droplet 4 has a slower velocity than droplets 2 and 3 that preceded it. The drops move at different speeds and coalescence can take place. The drop pair 9-10 coalesces to form drop A (Figure 2:v-vi) and 12-13 coalesces to form drop C (Figure 2:ix-x). Drop pair A-11 further coalesce to form B (Figure 2:viii-ix). Thirteen individual drops were identified prior to the appearance of the larger drop (labelled 14) in the high speed jet.

The exact mechanism that gives rise to this thin high speed jet is not known as attempts to video into the cavity was not successful as there was insufficient lighting. A probable mechanism of this thin high speed jet is the formation of a thin ejecta spray [12]. Weiss and Yarin[12] showed that during the first millisecond of contact between the drop and the impact surface, a thin axisymmetric ejecta sheet arises travelling horizontally to the impact surface and subsequently evolving into a range of shapes [11]. Thoroddsen has shown experimentally that such an ejecta sheet can have an initial speed more than 10 times the drop impact velocity. During the contact of the cavity walls to form the entrapped bubble, the impact is similar to that of a drop impact on a surface where the ejecta sheet is formed. In this case, the collapsing cavity is focussing towards a central point and the ejecta sheet formed reduces to an axisymmetric jet. This is observed as the thin high speed jet and precedes the high speed jet, which is formed by the large bulk of the fluid behind the impact point being re-directed up and downwards after impact.

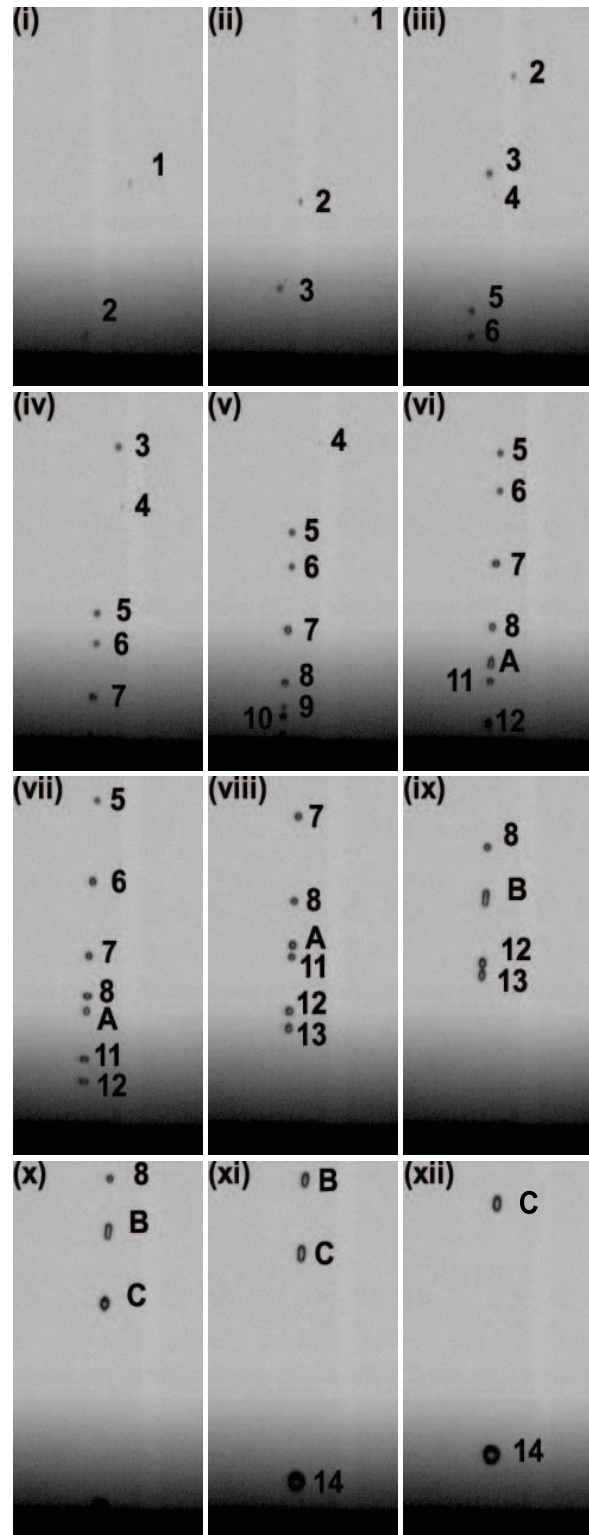


Figure 2: A sequence of twelve images of the thin high speed jet at $100 \mu\text{s}$ interval (10000 fps). Weber = 100, Froude = 110. The individual drops are given numeric identities, while the coalesced drops are given alphanumeric identities. The first frame start at 13.7 ms after drop impact.

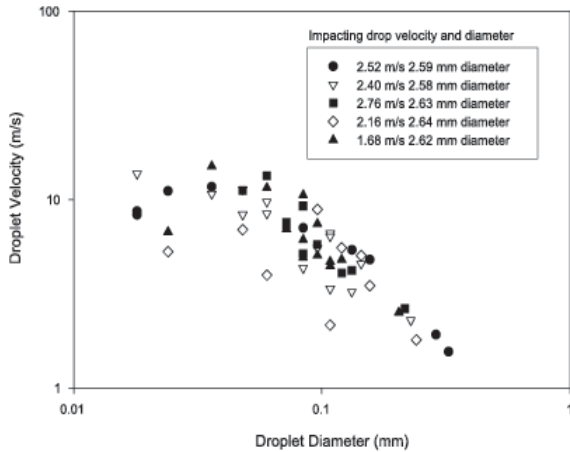


Figure 3: Droplet speed versus diameter from five different drop impacts. Each drop impact gives rise to 10-15 droplets.

Figure 3 shows a plot of the droplet diameter versus speed obtained from a number of observations. The speed was taken between the earliest two frames that the droplet was seen to emerge above the free surface, *i.e.* prior to coalescing if the droplets coalesced. The speed decreases logarithmically with the droplet diameter for droplet diameters larger than $100 \mu\text{m}$. For smaller droplet diameters, there is a large spread in the speeds measured and the results suggest that the droplet speed is independent of the droplet diameter. There is a gap between the 150 and $200 \mu\text{m}$ where no droplets having those diameters were found. A larger drop impact sample would be required to ascertain if this anomaly actually exists or just due to the small sample size. In the analysis of the droplet diameters and speed, it was found that the small fast moving droplets tend to be clustered together at the beginning and are skewed in shape while in flight. Moreover, the string of droplets does not rise vertically from the cavity, but rather the first few droplets are ejected at an angle from the axis of symmetry. After a short time, $\approx 600 \mu\text{s}$, the following droplets start to rise vertically from the cavity. This was found in all the experimental videos obtained so far.

Bubble Entrapment

The impact of the walls to entrap a bubble results in a high speed jet. It is expected that an equal but opposite jet should result, travelling downwards with the entrapped bubble. Although [1] alluded to the presence of a downward jet, they provided no evidence of it. Figure 4 shows the presence of the downward jet. The downward jet reaches the opposite surface of the entrapped bubble but does not penetrate it. The tip of the downward jet detaches to form a water droplet within the bubble. The downward jet does not always follow a vertical downward path and can be angled up to 45° in any direction from the vertical. Previous observations of this phenomena has only been observed using glycerol mixtures to slow down the bubble collapse phase (Lohse [3]) suggesting that the time scale for the process is strongly viscosity dependent. This phenomena has a number of similarities with the detachment of an air bubble formed at an orifice. Under certain conditions, a water jet penetrates into the bubble that is detached from a nozzle [4]. The acoustic signal emanated from the entrapped bubble has been used by Pumphrey and Elmore [8] to locate the region where bubble entrapment occurs, and [4] has used the detaching bubble acoustic to determine the size of the bubble formed from nozzles in industrial processes. However, for the bubble detaching from a nozzle, there has not been any reports of whether a

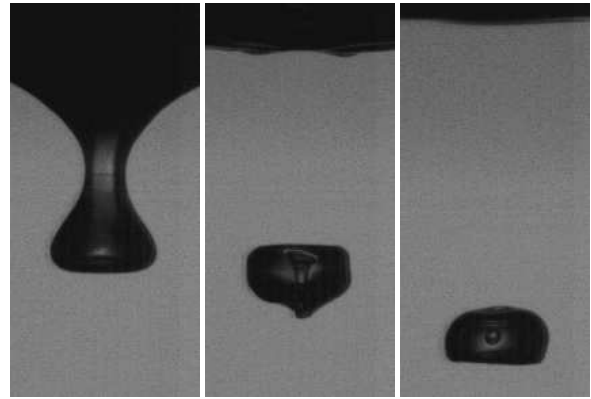


Figure 4: Three frames from a sequence showing the detachment of the entrapped bubble captured at 10000 fps. (Left) Cavity shape prior to snap off. (Middle) A jet penetrates the entrapped bubble $500 \mu\text{s}$ after snap off. (Right) Jet breaks up with a drop (diameter of $140 \mu\text{m}$) detached from the tip, $600 \mu\text{s}$ after snap off.

high speed jet is formed that travels back into the nozzle.

In some cases where the jet did not extend to the lower extremity of the air bubble, the jet would rapidly retract without leaving any fluid entrapped in the bubble. When the jet did break up in the entrapped drop, the length of the jet exceeded Rayleigh's wavelength of instability, $\lambda = 4.508D$, where D is the diameter of the downward jet. From the middle image in Figure 4 the diameter of the jet was estimated to be $108 \mu\text{m}$ resulting in $\lambda = 487 \mu\text{m}$. The length of the jet in this case is $528 \mu\text{m}$ thereby satisfying the conditions for instability and resulting in the jet breaking up. The size of the entrapped droplet that detached from the downward jet is shown in the right image in Figure 4 and is approximately $144 \mu\text{m}$ in diameter.

Figure 5 shows the subsequent motion of the drop within the entrapped bubble. The drop bounces inside the bubble before coalescing with the bulk fluid. The coalescing gives rise to a capillary wave that propagates over the bubble surface as well as a smaller secondary drop. The formation of progressively smaller drops during the coalescence process has been documented by Thoroddsen [10] for a drop on a flat liquid surface. The disturbance is quickly damped out and the air bubble returns to its spherical shape. The secondary drop remains visible for a moment before coalescing with the bulk fluid. This coalescing process again propagates a capillary wave over the bubble surface but of reduced amplitude and without any further drop formation. Elmore *et al.*[1], using dyed impacting drops, claimed that the downward jet consisted of the impacting fluid. This would suggest that the drop formed within the bubble consists of the impacting drop fluid. In the current experiments, some of the impacting drops were dyed but the backlighting used did not allow a conclusive determination of the source of the fluid of the drop formed in the bubble.

Thoroddsen[10] suggested that the process of one droplet coalescing and spawning a secondary drop is controlled by a dimensional similarity given by a constant $We = d^3/L^3$, where d is the diameter of the first drop formed and L is the diameter of the second drop formed. In this study, for every case where the secondary drop was produced and could be measured, the secondary drop was always found to be close to half the diameter of the first drop giving a constant $We = 8$.

The bubble entrapment process is extremely rapid. The camera was set to 30000 fps (128×136 pixels) in an attempt to capture

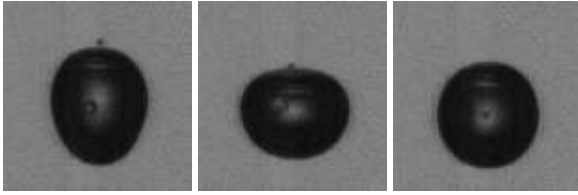


Figure 5: (Left) Formation of a liquid drop within the gas bubble. Entrapped drop $\approx 96 \mu\text{m}$ (Middle) Exact moment of coalescence 3.9 ms after the first appearance of the primary entrapped drop (Right) Secondary entrapped drop dia. $48 \mu\text{m}$. Bubble size is $\approx 660 \mu\text{m}$

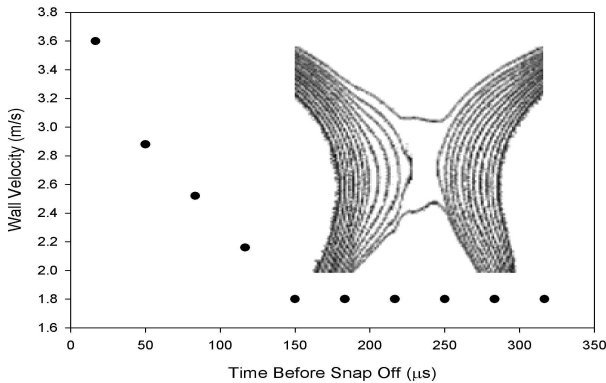


Figure 6: Cavity wall velocity versus time taken at 30000 fps tracking the velocity of the walls prior to bubble entrapment. Pixel outline of cavity walls prior to snap off shown in inset.

the evolution of the cavity walls prior to bubble entrapment. Figure 6 shows the velocity of the collapsing cavity walls moments before bubble entrapment. Approximately $150 \mu\text{s}$ before bubble break off, the left side of the cavity rapidly increases in velocity while the right side retains at a constant velocity. These actions result in an asymmetric acceleration of the cavity walls prior to bubble entrapment. To examine in more detail how the bubble snap off, the camera was set to 100000 fps (32×24 pixels). However, using such a low resolution meant that the evolution of the cavity profile in the moments before snap off could not be tracked. The smallest wall to wall distance prior to bubble entrapment captured was $72 \mu\text{m}$. This is almost half the distance of $156 \mu\text{m}$ from the 30000 fps sequence. The snap off of the bubble occurs in less than $10 \mu\text{s}$, in agreement with the fact the timescale for the snap off process is of the order of 0.2 ns. However, the local asymmetry of the cavity is a departure from most events involving liquid drop breakup problems. For example the break up of a liquid jet or snap off of a drop are axisymmetric. This implies that the cavity undergoes significantly more deformation before snap off than is described in the 30000 fps sequence. Therefore, to further understand how bubble entrapment actually occurs framing rates in excess of 100000 fps with greatly improved resolution would be required.

Conclusions

This study has sought to gain a deeper understanding of the fluid mechanics occurring during bubble entrapment using high-speed video photography with framing rates of 10000-100000 fps. Analysis of the high speed jet showed that a string of smaller high speed droplets preceded the high speed jet with speeds 50% greater than those for the high speed jet breakup. These droplets were an order of magnitude smaller than what had been observed before. It was concluded that these smaller

high speed droplets were the result of a focussing of the ejecta sheet into a thin high speed jet. This thin high speed jet then broke up rapidly on formation and cannot be observed above the bath free surface.

During the entrapment of the air bubble, the cavity walls were found to accelerate inwards in an asymmetric fashion where the left wall accelerated faster, relative to the centre line, than the right wall in the last $150 \mu\text{s}$ before bubble snap off. A high speed downward jet was observed in many cases of the entrapped bubble. If the high speed downward jet travelled far enough into the bubble, it broke up to form a single drop within the bubble. The bubble then bounced around the bubble until it coalesced with the bulk liquid through a coalescence cascade with a geometric similarity given by $We = 8$.

Acknowledgements

The equipment for this study was funded through an ARC LIEF grant.

References

- [1] Elmore, P. A., Chahine, G. L. and Oğuz, H. N., Cavity and flow measurements of reproducible bubble entrainment following drop impacts. *Exp. Fluids*, **31**, 2001, 664–673.
- [2] Liow, J.L., Splash Formation by spherical drops, *J. Fluid Mech.*, **427**, 2001, 73–105.
- [3] Lohse, D. Bubble puzzles. *Physics Today*. **56(2)**, 2003, 36–41.
- [4] Manasseh R., Yoshida, S. and Rudman, M., Bubble formation processes and bubble acoustic signals. *Third International Conference on Multiphase flow*, 1998, Lyon, France, June 8-12.
- [5] Manzello, S.L., Yang, J.C. and Cleary, T.G. On the Interaction of a Liquid Droplet with a Pool of Hot Cooking Oil, *Fire Safety Journal*, **38(7)**, 2003, 651–659.
- [6] Morton, D. E., Rudman, M. J. and Liow, J. L., An investigation of the flow regimes resulting from splashing drops. *Phys. Fluids*, **12**, 2000, 747–763.
- [7] Oğuz H. N. and Prosperetti, A., Bubble entrainment by the impact of drops on liquid surfaces. *J. Fluid Mech.*, **219**, 1990, 143–179.
- [8] Pumphrey, H. C. and Elmore, P. A., The entrainment of bubbles by drop impacts. *J. Fluid Mech.*, **220**, 1990, 145–165.
- [9] Rein, M., The transitional regime between coalescing and splashing drops, *J. Fluid Mech.*, **306**, 1996, 145–165.
- [10] Thoroddsen, S. T., and Takehara, K., The coalescence cascade of a drop. *Phys Fluids*, **12(6)**, 2000, 1265–1267.
- [11] Thoroddsen, S. T., The ejecta sheet generated by the impact of a drop. *J. Fluid Mech.*, **451**, 2002, 373–381.
- [12] Weiss, D. A. and Yarin, A. L., Single drop impact onto liquid film: neck distortion, jetting, tiny bubble entrainment, and crown formation. *J. Fluid Mech.*, **385**, 1999, 229–254.
- [13] Worthington, A.M., On impact with a liquid surface. *Proc. Roy. Soc.*, **34**, 1882, 217–230.
- [14] Zeff, B.W., Kleber, B., Fineberg, J. and Lathrop, D.P., Singularity dynamics in curvature collapse and jet eruption on a fluid surface, *Nature*, **403**, 2000, 401–404.